Structures and Reactivity of Binuclear Nickel(II) Complexes of 5,5-Bis(4′-amino-2′-azabutyl)-3,7-diazanonane-1,9-diamine†

Alexander McAuley,* Kathy Beveridge, S. Subramanian and Todd W. Whitcombe
Department of Chemistry, P.O. Box 1700, University of Victoria, Victoria, B.C. V8W 2Y2, Canada

Three different forms of binuclear nickel(II) complexes of the acyclic polyamine ligand, 5,5-bis(4′-amino-2′-azabutyl)-3,7-diazanonane-1,9-diamine (tabm) have been prepared and characterised structurally by X-ray crystallography. The complex $[Ni_2(tabm)][ClO_4]_4 \cdot H_2O$ (space group $P2_1/c$, monoclinic, $a = 21.884(4)$, $b = 8.349(3)$, $c = 16.852(3)$ Å, $\beta = 96.88(2)°$, $R = 0.0733$, $R' = 0.0875$) has both nickel(II) centres in a square-planar geometry. In $[(NiCl_2)_2(tabm)] \cdot 2H_2O$ [space group $P\bar{1}$ (no. 2), triclinic, $a = 8.637(2)$, $b = 22.106(7)$, $c = 6.812(2)$ Å, $\alpha = 94.95(7)°$, $\beta = 106.25(3)°$, $\gamma = 93.78(4)°$, $R = R' = 0.0496$) both the nickel(II) centres are octahedral. The third structure is of the novel complex $[Ni_2Cl(OH_2)(tabm)][ClO_4]_3 \cdot H_2O$ [space group $P2_12_12_1$ (no. 19), orthorhombic, $a = 13.734(3)$, $b = 16.645(4)$, $c = 13.021(3)$ Å, $R = 0.0648$, $R' = 0.070$] in which there is present in the same cation both a square-planar and an octahedral nickel(II) centre. The bond lengths and angles for the square-planar NiN_4 moieties provide evidence for an 'ideal' Ni–N bond length which is based on an analysis of the present and other similar data. The ligand tabm in these complexes has two tetraaza units emanating from a single carbon which are paired in a rigid, nearly orthogonal orientation. As a result, the complexes show extraordinary kinetic stability in acidic media relative to 3,7-diazanonane-1,9-diaminenickel(II). All three complexes may be oxidised to corresponding nickel(III) species which according to time-dependent ESR spectra undergo a gradual change in geometry to a single final solution configuration. The integrity of these structures in solution depends upon the nature of the solvent, as demonstrated by ultraviolet–visible and ESR spectroscopy. Cyclic voltammetry of $[Ni_2(tabm)]^{4+}$ in acetonitrile (0.1 mol dm^{-3} NEt_4BF_4) shows two waves, and from differential pulse polarography a comproportionation constant ($K_c = 72.5$) for the mixed-valence ($Ni^{II}Ni^{III}$) species was evaluated.

Binuclear complexes containing two similar (homo) or two dissimilar (hetero) metal ions are important in the modelling of biological systems,[1] in the study of metal–metal (electronic and magnetic) interactions,[2,3] and in the activation of small molecules.[4,5] A variety of binuclear systems have been synthesised and characterised structurally.[3,6–8] The reactivity of metal ions in such complexes has been shown to be dependent upon the distance between the metal centres,[9,10] types of bridging ligands and also on the relative orientations of the metal ions.[11] Complexes have been prepared in which either a single large framework wraps around two metal ions, as for example, in polyketonates[12] and large macrocycles[13] or in two independent ligating entities joined together by a bridging group.[14–16] These complexes contain open-chain or macrocyclic ligands with or without bridging atoms. Thus, the nature and extent of interaction between the metal ions are controlled principally by the ligand structure.

There are only a few complexes known in which the orientation of the metal ions is very rigidly controlled. Most of these are metalloporphyrins synthesised to model natural photosynthetic systems.[17–19] Also, a few synthetic macrocyclic complexes have been reported in which a well defined orientation of metal centres has been achieved.[20,21] The binucleating ligand 5,5-bis(4′-amino-2′-azabutyl)-3,7-diazanonane-1,9-diamine[tetrakis(4-amino-2-azabutyl)methane, tabm] described herein is relatively unexplored[22] in its metal complexes, compared to its parent analogue 3,7-diazanonane-1,9-diamine. The latter ligand is a precursor to 1,4,8,11-tetraazacyclotetradecane (cyclam) and is one of the well studied linear tetraamines. Complexes with Ni^{II}, Cu^{II}, Co^{III} and Cr^{III} have been described.[23] The open-chain amine tabm may be viewed as a derivative of 3,7-diazanonane-1,9-diamine in which the central carbon of the trimethylene bridge is substituted with two (4-amino-2-azabutyl) chains. The resulting octaaza ligand can function potentially in two different co-ordination modes as shown in I and II.

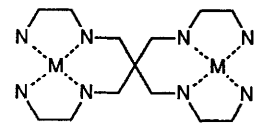

I

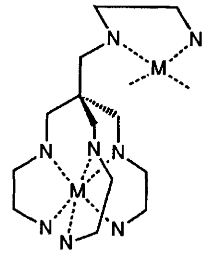

II

In structure I two MN_4 chromophores are formed and in II a cage type MN_6 chromophore and a MN_2 chelate ring are identified. The mode of complexation is determined largely by the nature and geometric preferences of the transition-metal ion, but is also dependent upon the methods of preparation.[24] The present paper reports an investigation into the chemistry of the nickel(II) complexes derived from tabm. In these complexes the structural rigidity of the ligand enforces a much stronger in-plane field than 3,7-diazanonane-1,9-diamine, resulting in a higher kinetic stability and facilitating oxidation of the metal centre to form nickel(III) complexes.

Earlier studies[22] and a recent investigation by Gahan *et al.*[25] have reported on the preparation of the ligand tabm and of the

---

† *Supplementary data available:* see Instructions for Authors, *J. Chem. Soc., Dalton Trans.*, 1991, Issue 1, pp. xviii–xxii.

Non-SI units employed: G = 10^{-4} T, cal = 4.184 J.

corresponding copper(II) complex ions. There is evidence from ESR data, using the $[Cu_2(tabm)]^{4+}$ cation, of interaction between the two copper centres. Although a redox wave is observed for these Cu^{II}–Cu^{I} couples in aqueous media, this behaviour is limited generally to non-aqueous conditions for generating higher oxidation states, in view of the ready hydrolysis in acidic media of metal complexes involving co-ordinated primary amines. Although this problem may be overcome to a large extent by use of complexes of macrocyclic ligands, the nickel(II) complexes of tabm described in this study possess properties not shown by the parent complex of 3,7-diazanonane-1,9-diamine and, in general, by many nickel(II) complexes of open-chain amines. X-Ray crystal structures of the hydrochloride[26] salt of tabm and of a binuclear nickel(II) complex of the macrocyclic C-spiro-bicyclam analogue (L^1)[21] have been reported elsewhere.

An additional interest in the present systems arises from the fact that more data are becoming available from X-ray studies on Ni^{II}–N bond lengths for the square-planar low-spin configuration in both macrocyclic and acyclic complexes. Molecular mechanics calculations on optimal distances have been reported recently[27,28] for high- and low-spin nickel(II) species. For square-planar nickel(II) in the *trans* III configuration with tetraazacyclotetradecane ([14]aneN_4) macrocycles an ideal Ni–N bond length of 1.89–1.90 Å has been proposed.[29] The present data provide evidence for values somewhat longer (1.945 Å) in a closely related family of cations, where in some cases there is the opportunity for the system to adopt a geometry free from steric constraints.

Experimental

Synthesis.—The complexes described were prepared by reaction of $[Ni(H_2O)_6]^{2+}$ with the mixture of ligands obtained from the reaction of ethylenediamine with pentaerythrityl tetrabromide [1,3-dibromo-2,2-bis(bromomethyl)-propane]. Details of their preparation and isolation have been reported recently.[26] Only a brief account of the preparation and crystallisation of the different forms is presented in the context of X-ray crystallographic characterisation and the study of the properties of these complexes.

$[(NiCl_2)_2(tabm)]\cdot 2H_2O$. This complex was obtained as one of the fractions from a mixture of nickel(II) complexes prepared using the procedures previously described.[26] The fraction was concentrated and extracted with methanol to remove most of the sodium chloride used as an eluent in the cation-exchange chromatography. The violet methanolic extract was cooled to precipitate the remaining traces of sodium chloride and concentrated to dryness. The resulting solid was extracted with 90% ethanol and the ethanolic extracts concentrated and allowed to stand. Pale violet crystals of the bis(octahedral) complex were obtained. X-Ray quality crystals were obtained by diffusing diethyl ether into a solution of this complex in 90% ethanol [Found: C, 27.45; H, 6.25; Cl, 25.35; N, 19.50. Calc. for $C_{13}H_{36}Cl_4N_8Ni_2$ (anhydrous): C, 27.70; H, 6.40; Cl, 25.20; N, 19.90%].

Yields were dependent upon the efficiency of extraction from sodium chloride with which the crude complex was invariably found to be contaminated.

$[Ni_2(tabm)][ClO_4]_4\cdot H_2O$. **CAUTION.** Transition-metal perchlorates are hazardous and may explode. Only small quantities should be prepared and great care taken.

To a concentrated methanolic solution of the chloro-complex described above, a saturated aqueous solution of $NaClO_4$ was added and the solution left to stand. Yellow microcrystals of the perchlorate salt of the cation $[Ni_2(tabm)]^{4+}$ were precipitated. The complex was recrystallised from water containing sodium perchlorate to yield a monohydrate (Found: C, 18.60; H, 4.50; N, 13.25; Ni, 13.90. Calc. for $C_{13}H_{38}Cl_4N_8Ni_2O_{17}$: C, 18.65; H, 4.55; N, 13.35; Ni, 14.00%).

X-Ray quality crystals were obtained by allowing a dilute solution of the complex to stand for some days in large volumes of a saturated solution of sodium perchlorate.

$[Ni_2Cl(OH_2)(tabm)][ClO_4]_3\cdot H_2O$. Crystals of this complex were obtained from the mother-liquor after removal of the microcrystalline precipitate of $[Ni_2(tabm)][ClO_4]_4\cdot H_2O$. The complex crystallised as a monohydrate. However, the crystals were found to be efflorescent and the water of crystallisation was lost readily. Hence, only the anhydrous form was analysed (Found: C, 20.05; H, 4.85; N, 14.20. Calc. for $C_{13}H_{38}Cl_4N_8Ni_2O_{13}$: C, 20.15; H, 4.90; N, 14.50%).

Crystallography.—Experimental parameters for the three crystals are listed in Table 1. Crystals were mounted inside a glass Lindemann tube using epoxy resin and the unit-cell dimensions and space groups determined by use of Weissenberg and procession photography, after which the crystals were transferred to a Picker four-circle diffractometer automated with a PDP11/10 computer. In the case of the bis(square-planar) complex, measurements were obtained using a Nonius-Enraf CAD 4 system.

$[(NiCl_2)_2(tabm)]\cdot 2H_2O$. The unit cell was refined using 12 pairs of reflections in the 2θ range 25–45°. Intensity measurements were obtained by scanning in the θ–2θ mode using 160 steps of 0.01° in 2θ, counting for 0.25 s per step. Background counting was introduced for 20 s at the end of each scan. A set of three standard reflections preceded each batch of 50 measurements, with no noticeable change in intensity observed during collection.

Solution of the phase problem was achieved by direct methods using SHELX 76.[30] The atomic scattering factors were those included in the compilation of Cromer and Mann[31] together with the nickel f curve.[32] The program used for absorption correction was a local modification of an existing procedure.[33] The structure was refined using least-squares techniques in SHELX 76.[30] All atoms were refined anisotropically except for the hydrogens which were not resolved. The refinement converged with a maximum shift/estimated standard deviation (e.s.d.) of 0.085. The maximum peak in the difference map was 0.875 e $Å^{-3}$. A unit weighting scheme was used with 4608 ($I > 3\sigma I$) of the 5691 observed reflections and 262 parameters.

$[Ni_2(tabm)][ClO_4]_4\cdot H_2O$. The lattice parameters were obtained from a least-squares refinement of 15 accurately centred, high-angle reflections. The space group was confirmed by the collection of both the $0k0$ and $h0l$ reflections where the expected systematic absences occurred. A prescan and a variable-speed final scan were used during data collection, a set of three standards were measured hourly, and the orientation checked after every 500 reflections.

The structure was solved for the heavy atoms using MULTAN[34] and refined by least squares using SHELX 76.[30] Details of atomic scattering factors and absorption corrections are as given above. All non-hydrogen atoms were located from Fourier difference maps. Owing to the large number of atoms in the asymmetric unit (44), a blocked matrix was used in the final stages of convergence. Both blocks contained the two nickels and the four chlorine atoms (55 parameters), while the oxygen atoms (153 parameters) and the carbon and nitrogen atoms (189 parameters) were separated. Some of the hydrogen atoms were located from the difference maps but were included in calculated positions in the final stages of refinement with a common isotropic thermal parameter. The final difference map had a maximum peak height of 0.85 e $Å^{-3}$. Of the 2754 reflections collected 2395 ($I > 3\sigma I$) were used. Weights were obtained from counting statistics using $w = 1/[\sigma^2(F) + 0.10F^2]$.

$[Ni_2Cl(OH_2)(tabm)][ClO_4]_3\cdot H_2O$. The unit cell was refined using 18 pairs of reflections in the θ–2θ range 19–40°. The intensity measurements were obtained by scanning in the θ–2θ mode using 160 steps of 0.01° in 2θ, counting for 0.25 s per step. Background counting was introduced for 20 s at the end of each

Table 1 Crystallographic data

	$[Ni_2(tabm)][ClO_4]_4 \cdot H_2O$	$[(NiCl_2)_2(tabm)] \cdot 2H_2O$	$[Ni_2Cl(OH_2)(tabm)][ClO_4]_3 \cdot H_2O$
Molecular formula	$C_{13}H_{38}Cl_4N_8Ni_2O_{17}$	$C_{13}H_{40}Cl_4N_8Ni_2O_2$	$C_{13}H_{40}Cl_4N_8Ni_2O_{14}$
M	839.7	599.69	791.6
Crystal colour	Orange-yellow	Lilac	Reddish brown
Crystal system	Monoclinic	Triclinic	Orthorhombic (non-centrosymmetric)
Space group	$P2_1/c$	$P\bar{1}$ (no. 2)	$P2_12_12_1$ (no. 19)
a/Å	21.884(4)	8.637(2)	13.734(3)
b/Å	8.349(3)	22.106(7)	16.645(4)
c/Å	16.852(3)	6.812(2)	13.021(3)
α/°		94.95(7)	
β/°	96.88(2)	106.25(3)	
γ/°		93.78(4)	
U/Å^3	3057	1238.5	2976.6
D_c/g cm^{-3}	1.835	1.604	1.753
D_m/g cm^{-3}	1.820	1.608	1.766
Z	4	2	4
μ/cm^{-1}	16.6	18.97	17.09
$F(000)$	1695.90	667.95	1559.90
Scan width	0.8 + 0.2 tanθ		
Transmission coefficient	0.536–0.750	0.576–0.663	0.476–0.532
$R(F_o)$	0.0733	0.0496	0.0648
R'	0.0875	0.0496	0.070

scan. A set of three standard reflections preceded each batch of 50 measurements, with no noticeable change in intensity observed during collection. Weights were obtained using $w = 1/[\sigma^2(F) + 0.0010F^2]$.

Solution of the phase problem was achieved using MULTAN.[34] Details of atomic scattering factors and absorption corrections are as given above. The structure was refined using least-squares techniques with SHELX 76.[30] All atoms were refined anisotropically except for the hydrogens of which only two (those of the co-ordinated water molecules) were refined. The refinement converged with a maximum shift/e.s.d. of 0.1 for all atoms except O(1)(0.96) and H(2)(1.2). The maximum peak height in the difference map was 1.1 e Å^{-3}. Of the 3848 observed reflections, 3092 ($I > 3\sigma I$) were used.

Additional material for each structure available from the Cambridge Crystallographic Data Centre comprises H-atom coordinates, thermal parameters and remaining bond lengths and angles.

Physical Measurements.—All chemicals were of reagent quality used without any further purification.

Ultraviolet–visible spectra were obtained in quartz cells using a Perkin-Elmer Lambda 4B spectrometer equipped with a Haake D8 thermostat. Limiting values of ε for the square-planar complexes were obtained in nitromethane solution. Equilibrium constants were calculated using the expression $K = \varepsilon_T/(\varepsilon_{limit} - \varepsilon_T)$ where ε_{limit} is the absorption coefficient for the 100% square-planar form and ε_T that for the square-planar form at temperature T. Solutions were allowed to equilibrate for at least 20 min at each temperature prior to measurements being made.

The ESR spectra were recorded on a Varian E-6S X-band spectrometer at 77 K. Frozen matrices were prepared by rapid cooling of solutions in liquid N_2. The reference used was diphenylpicrylhydrazyl (dpph) ($g = 2.0037$). Solutions containing the oxidised nickel ion were prepared either by reaction with $Na_2S_2O_8$ in neutral aqueous media or by use of $NOBF_4$ in non-aqueous media.

Cyclic voltammetric measurements were made using a PAR model 273 potentiostat/galvanostat connected to an IBM personal computer and polarographic measurements by use of a Metrohm 626 Polarecord instrument. A three-electrode cell configuration consisting of platinum working electrodes was used. For aqueous measurements a saturated calomel electrode (SCE) was used as a reference electrode. For non-aqueous measurements a reference system of Ag–Ag$^+$ (0.01 mol dm^{-3})/NEt_4BF_4 (0.10 mol dm^{-3}) in MeCN was employed with the ferrocene–ferrocenium couple used as an external standard.[35] The salts $LiNO_3$, LiCl and $LiClO_4$ used as supporting electrolytes in aqueous media were doubly recrystallised from deionised water and NEt_4BF_4 was crystallised twice from a mixture of alcohol and diethyl ether. The electrolyte solutions were purged with argon and an atmosphere of this gas was maintained during electrochemical measurements.

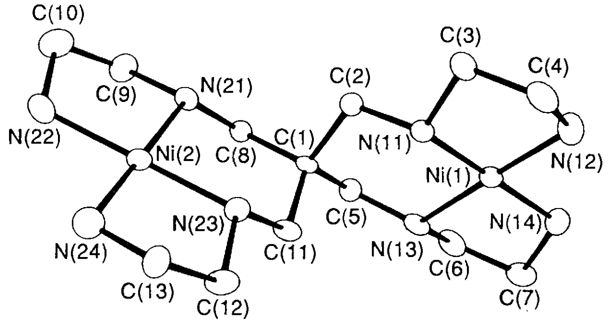

Fig. 1 Molecular structure of the cation $[Ni_2(tabm)]^{4+}$ showing 25% thermal ellipsoids

Results

The ORTEP diagrams of the complex cations $[Ni_2(tabm)]^{4+}$ and $[Ni_2Cl(OH_2)(tabm)]^{3+}$ and that of the neutral complex $[(NiCl_2)_2(tabm)]$ are shown in Figs. 1–3. The fractional coordinates, bond lengths and angles are included in Tables 2 and 3, 4 and 5, and 6 and 7 respectively. The Ni–N bond lengths are consistent with previous observations relating to high- and low-spin Ni^{II} (Table 8). From the values included in Table 8, a value of 1.95(2) Å is suggested as diagnostic of the square-planar d^8 centre. Ultraviolet–visible spectroscopic data in various solvents are presented in Table 9. Temperature-dependence studies have been carried out in order to determine relative ratios of the high-spin:low-spin forms in solution and the thermodynamic parameters derived therefrom are compared with similar complexes in Table 10. Oxidation by NO$^+$ in MeCN or $S_2O_8^{2-}$ in aqueous media results in nickel(III) complexes which have been characterised. Using the latter reagent at neutral pH, metal-based paramagnetic species are

Table 2 Fractional atomic coordinates (× 10^5 for Ni, × 10^4 for others) for $[Ni_2(tabm)][ClO_4]_4\cdot H_2O$ with e.s.d.s in parentheses

Atom	*X*/*a*	*Y*/*b*	*Z*/*c*
Ni(1)	12 487(6)	35 794(17)	38 831(8)
Ni(2)	37 282(6)	2 143(17)	30 067(9)
Cl(1)	8 493(2)	2 214(3)	9 833(2)
Cl(2)	6 151(2)	3 393(5)	5 476(3)
Cl(3)	3 607(2)	3 918(4)	1 741(2)
Cl(4)	9 219(2)	5 752(5)	2 753(2)
N(11)	1 927(4)	3 691(10)	3 261(5)
N(12)	907(5)	5 381(14)	3 256(6)
N(13)	1 600(4)	1 779(10)	4 507(5)
N(14)	552(4)	3 441(13)	4 466(7)
N(21)	3 792(4)	1 723(11)	3 882(6)
N(22)	4 610(5)	113(15)	3 216(7)
N(23)	2 842(4)	337(11)	2 811(5)
N(24)	3 684(5)	−1 185(12)	2 102(7)
C(1)	2 651(5)	1 783(11)	4 064(6)
C(2)	2 567(4)	3 461(12)	3 662(6)
C(3)	1 882(6)	5 303(15)	2 812(7)
C(4)	1 235(6)	5 570(16)	2 581(8)
C(5)	2 268(5)	1 719(12)	4 751(7)
C(6)	1 252(6)	1 695(17)	5 234(7)
C(7)	585(6)	1 990(18)	4 959(8)
C(8)	3 301(5)	1 631(12)	4 466(6)
C(9)	4 409(6)	1 554(17)	4 346(9)
C(10)	4 841(6)	1 415(19)	3 734(10)
C(11)	2 481(5)	378(12)	3 482(7)
C(12)	2 622(5)	−1 018(16)	2 231(8)
C(13)	3 058(6)	−1 091(17)	1 640(8)
O(11)	8 383(6)	2 999(11)	545(6)
O(12)	8 265(6)	2 989(14)	−856(7)
O(13)	8 219(5)	558(12)	−140(6)
O(14)	9 130(5)	1 921(16)	−117(8)
O(21)	5 712(9)	2 290(20)	5 471(14)
O(22)	6 047(7)	4 728(18)	5 846(10)
O(23)	6 670(11)	2 861(26)	5 888(33)
O(24)	6 084(26)	4 159(49)	4 706(23)
O(31)	2 988(7)	3 224(18)	1 723(8)
O(32)	3 587(8)	5 261(21)	1 277(12)
O(33)	3 893(10)	4 090(31)	2 495(7)
O(34)	3 972(11)	2 906(32)	1 354(13)
O(41)	8 648(4)	6 413(14)	2 966(5)
O(42)	9 636(7)	6 905(19)	2 504(13)
O(43)	9 524(6)	4 858(21)	3 361(9)
O(44)	9 060(9)	4 700(29)	2 145(12)
O(1)	4 942(8)	4 142(31)	6 661(12)

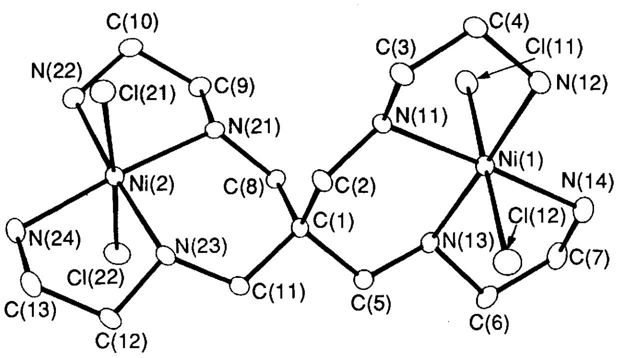

Fig. 2 Molecular structure of the complex $[(NiCl_2)_2(tabm)]$ showing 25% thermal ellipsoids

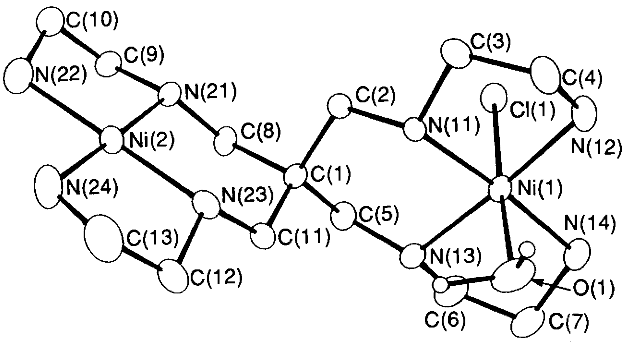

Fig. 3 Molecular structure of the cation $[Ni_2Cl(OH_2)(tabm)]^{3+}$ showing 25% thermal ellipsoids

observed with $g_\perp = 2.180$ and $g_\parallel = 2.02$, consistent with axial symmetry. In electrochemical studies in acetonitrile, evidence has been obtained for two consecutive one-electron oxidations, with a comproportionation constant for the mixed-valence intermediate of 72.5. Details of these results are presented in the tables and in the following sections.

Crystal Structures.—Although the three complexes described are formed from the same ligand but with different co-ordination geometries, there are resemblances within the ligand framework. The structures of the individual complexes are discussed first and common structural features compared briefly.

Table 3 Interatomic distances (Å) and angles (°) for $[Ni_2(tabm)]$-$[ClO_4]_4\cdot H_2O$ with e.s.d.s in parentheses

N(11)–Ni(1)	1.920(10)	N(21)–Ni(2)	1.932(10)
N(12)–Ni(1)	1.936(11)	N(22)–Ni(2)	1.921(11)
N(13)–Ni(1)	1.939(8)	N(23)–Ni(2)	1.930(9)
N(14)–Ni(1)	1.914(11)	N(24)–Ni(2)	1.914(11)
N(12)–Ni(1)–N(11)	86.4(4)	N(14)–Ni(1)–N(13)	87.9(4)
N(13)–Ni(1)–N(11)	93.0(4)	N(22)–Ni(2)–N(21)	84.8(5)
N(13)–Ni(1)–N(12)	179.3(4)	N(23)–Ni(2)–N(21)	94.3(4)
N(14)–Ni(1)–N(11)	177.7(4)	N(23)–Ni(2)–N(22)	179.1(5)
N(14)–Ni(1)–N(12)	92.8(5)	N(24)–Ni(2)–N(21)	176.6(4)
N(24)–Ni(2)–N(23)	86.7(4)	N(24)–Ni(2)–N(22)	94.2(5)

$[Ni_2(tabm)][ClO_4]_4\cdot H_2O$. The cation contains two identical NiN_4 chromophores, each of which may be viewed as a 3,7-diazanonane-1,9-diaminenickel moiety joined at a single carbon (Fig. 1). In each NiN_4 chromophore, the nickel and the four nitrogens are coplanar with an average Ni–N distance of 1.934(10) Å. The two nickel centres are separated by a distance of 6.437 Å and the two NiN_4 planes are 'quasi-orthogonal' to each other subtended by an angle of 83.2°. The nickel atoms are located at the centre of the rectangle described by the four nitrogens in each diazanonanediamine moiety. In both NiN_4 chromophores the distances between the primary nitrogens (2.788 and 2.809 Å) and those between the secondary nitrogens (2.798 and 2.831 Å) are similar.

The Cl–O bonds do not show any trends which reflect the co-ordination of an oxygen atom by a metal centre. Generally, such co-ordination to nickel results in the lengthening of the Cl–O bond[47] with much shorter Ni–O distances.[48] This has been observed for the axially bound ClO_4^- (Cl–O 2.085 Å) in $[Ni^{III}(cyclam)(ClO_4)_2]PF_6$.[37] However, the absence of any such features in the present structure is consistent with a crystalline complex containing two square-planar, low-spin d^8 nickel(II) centres.

$[(NiCl_2)_2(tabm)]$. This neutral complex contains two essentially identical NiN_4Cl_2 chromophores (Fig. 2) in which the nickel atoms and the nitrogens are coplanar and the chloride ions occupy the axial sites. An average Ni–N distance of 2.086(9) Å is observed while the Ni–Cl distances average 2.506(3) Å. The Ni–N distances in this complex are longer than

Table 4 Fractional atomic coordinates (× 10^5 for Ni and Cl, × 10^4 for others) for $[Ni_2Cl(OH_2)(tabm)][ClO_4]_3 \cdot H_2O$ with e.s.d.s in parentheses

Atom	*X*/*a*	*Y*/*b*	*Z*/*c*
Ni(2)	37 500(1)	8 750(1)	54 440(1)
Ni(1)	81 043(8)	−5 627(7)	45 230(9)
Cl(1)	81 693(19)	−833(17)	26 595(18)
Cl(2)	31 693(21)	6 839(19)	2 987(22)
Cl(3)	1 654(18)	24 061(17)	36 304(21)
Cl(4)	10 633(19)	22 919(16)	73 243(24)
O(21)	2 693(12)	900(12)	1 162(13)
O(22)	3 528(9)	−68(7)	170(22)
O(23)	3 887(10)	1 197(7)	12(12)
O(24)	2 379(12)	703(17)	−376(13)
O(31)	772(9)	3 060(8)	3 395(15)
O(32)	607(9)	1 663(7)	3 651(18)
O(33)	−323(21)	2 552(11)	4 510(20)
O(34)	−607(22)	2 281(18)	3 101(31)
O(41)	1 975(9)	2 560(7)	6 915(11)
O(42)	1 068(16)	2 427(10)	8 383(10)
O(43)	962(9)	1 467(7)	7 176(12)
O(44)	280(14)	2 681(14)	6 836(18)
O(1)	8 125(11)	−990(7)	6 123(7)
O(2)	3 845(19)	2 768(8)	−980(14)
N(11)	7 241(5)	373(4)	5 051(6)
N(12)	9 249(6)	202(7)	4 878(7)
N(13)	6 866(6)	−1 257(4)	4 219(6)
N(14)	8 894(7)	−1 577(6)	4 088(9)
N(21)	4 299(5)	906(4)	4 068(6)
N(22)	2 726(7)	1 560(7)	4 912(9)
N(23)	4 767(6)	217(5)	6 011(6)
N(24)	3 198(7)	874(7)	6 788(8)
C(1)	5 644(6)	−121(5)	4 340(7)
C(2)	6 360(6)	578(5)	4 430(6)
C(3)	7 895(8)	1 104(7)	5 101(11)
C(4)	8 875(8)	849(7)	5 551(9)
C(5)	6 060(7)	−836(5)	3 730(8)
C(6)	7 220(10)	−1 942(6)	3 593(10)
C(7)	8 133(10)	−2 277(7)	4 044(10)
C(8)	4 784(6)	189(6)	3 655(7)
C(9)	3 499(7)	1 168(6)	3 344(9)
C(10)	3 022(8)	1 842(7)	3 870(11)
C(11)	5 236(6)	−411(5)	5 356(7)
C(12)	4 373(8)	−171(8)	6 945(8)
C(13)	3 837(11)	496(11)	7 534(9)

those observed in the bis(square planar) cation $[Ni_2(tabm)]^{4+}$. In the octahedral cation the nickel centres are pushed towards the 'open' end of the diazanonanediamine moiety, widening the distance between the primary amino groups. This is reflected in the increased distance (0.29 Å) between the metal centres (6.727 Å). The presence of an octahedral nickel centre also results in a number of other structural changes. Within each NiN_4Cl_2 unit the distances between the primary nitrogens and those between the secondary nitrogens are 3.127 and 2.996 Å respectively. These are larger than similar distances (2.788 and 2.809 Å) observed in the NiN_4 units of the cation $[Ni_2(tabm)]^{4+}$. The larger size of the octahedral nickel ion is also reflected in the N–Ni–N angles. Those subtended by the secondary nitrogens at the nickel centres [N(11)–Ni(1)–N(13) and N(21)–Ni(2)–N(23)] are 93.1(2) and 91.9(2)° respectively. However, the angles involving the terminal primary amines [N(12)–Ni(1)–N(14) and N(22)–Ni–N(24)] are larger at 97.4(2) and 99.5(2)° respectively. The Cl–Ni–Cl angles are 179.0(1) and 176.0(4)° respectively. Similar values have been observed for the O–Cu–O angles in the analogous copper complex $[Cu_2(tabm)(NO_3)_4]$.[25]

$[Ni_2Cl(OH_2)(tabm)][ClO_4]_3 \cdot H_2O$. The structure of this cation (Fig. 3) is interesting in that there is present within the same cation both a square-planar and an octahedral nickel(II) centre. To the best of our knowledge, the only other complex of this type that has been characterised structurally has both square-planar NiN_2O_2 and octahedral NiN_2O_4 chromophores in an unsaturated ligand system.[49] The cation described here has the combined structural features of the bis(square planar) and bis(octahedral) cations described above. The differences observed between the square-planar and the octahedral nickel centres are again evident. The average Ni–N distances for the square-planar and octahedral nickel(II) segments are 1.925(9) and 2.085(8) Å respectively. As described earlier, the octahedral nickel is pushed slightly away from the centre of the rectangle described by the four nitrogen donors towards the open end of the diazanonenediamine moiety. The resulting effect is the same as that observed in the bis(octahedral) complex described above, The distance between the nickel centres is 6.552 Å. The angle [N(11)–Ni(1)–N(13)] subtended by the secondary nitrogens at the octahedral nickel centre is 90.7(3)°, while the primary amines subtend an angle [N(12)–Ni(1)–N(14)] of 99.4(4)°. However, in the square-planar NiN_4 unit, all four N–Ni–N angles are close to the expected values of 86.3(4)° for five- and 93.6(4)° for the six-membered chelate rings and the nickel atom is located at the centre of the rectangle described by the four donor nitrogens.

The three complexes described here have common structural features. A comparison of these features and their effects on the reactivity is of importance. The planes containing the four nitrogens and the nickel atoms are 'quasi-orthogonal' to each other, with this angle, as found in the bis(square planar) cation $[Ni_2(tabm)]^{4+}$, being 83.2°. The tilt in this angle from the 90° angle at the spiro carbon is the result of the chair conformation adopted by the six-membered chelate ring which contains the spiro carbon. This 'bent' geometry is also observed in the nickel(II) complex of the macrocyclic ligand C-spiro-bicyclam.[21]

Another feature is the intermetal distances in the three cations. The Ni • • • Ni distance is greater for the bis(octahedral) system, increasing from 6.437 Å in the bis(square planar) cation to 6.727 Å in $[Ni_2Cl_4(tabm)]$. An intermediate distance of 6.552 Å is observed in the cation with the mixed co-ordination geometry. The gradual increase in the intermetal distance does not appear to result from steric interactions from the axial ligands when the metal centres adopt an octahedral geometry.

In the cation $[Ni_2(tabm)]^{4+}$ the O(13) of one perchlorate has a interatomic distance of 2.826 Å to Ni(1) in one symmetry position, and O(33) of a different perchlorate is 3.380 Å from Ni(2) in another symmetry position. These distances are greater than the normally accepted values for Ni–O bonding[48] and are viewed as being the result of electrostatic interactions. Interestingly, in the structure[41] of $[Ni(Me_2[13]aneN_4)(ClO_4)_2]$($Me_2[13]aneN_4$ = 12,12-dimethyl-1,4,7,10-tetraazacyclotridecane) similar distances (2.86 and 3.19 Å) were observed between the nickel ion and the perchlorate oxygens. In the cation $[Ni_2Cl(OH_2)(tabm)]^{3+}$, distances of 2.912 and 3.232 Å may be observed from Ni(2) to the perchlorate oxygens O(24) and O(33), respectively. Presumably, again this is a result of electrostatic interactions between the Ni^{2+} ions and the perchlorate ions enhanced during crystallisation. Further examination of the unit cell indicates clearly that the octahedral metal centre is removed from any intermolecular contacts. The lower net surface charge (+1 spread over a large spherical surface area) diminishes electrostatic attractions.

While molecular mechanics calculations[28] indicate that the cavity size of cyclam is best suited for a high-spin nickel(II) ion with an ideal Ni–N distance of approximately 2.07 Å, the ideal Ni–N distance for a low-spin nickel(II) ion in tetraaza complexes has been a subject of debate. With a limited data set (entries **10**–**12** in Table 8), Fabbrizzi[29] proposed an ideal Ni–N distance of 1.89 Å for low-spin nickel(II) ions. This implies that cyclam is not suitable for this electronic configuration. However, stability

Table 5 Interatomic distances (Å) and angles (°) for $[Ni_2Cl(OH_2)(tabm)][ClO_4]_3{\cdot}H_2O$ with e.s.d.s in parentheses

N(21)–Ni(2)	1.945(8)	O(1)–Ni(1)	2.202(9)
N(22)–Ni(2)	1.938(10)	N(11)–Ni(1)	2.074(7)
N(23)–Ni(2)	1.922(8)	N(12)–Ni(1)	2.075(10)
N(24)–Ni(2)	1.907(10)	N(13)–Ni(1)	2.094(8)
Cl(1)–Ni(1)	2.556(3)	N(14)–Ni(1)	2.085(9)
N(22)–Ni(2)–N(21)	86.3(4)	N(12)–Ni(1)–N(11)	84.2(3)
N(23)–Ni(2)–N(21)	95.0(3)	N(13)–Ni(1)–Cl(1)	91.2(2)
N(23)–Ni(2)–N(22)	178.1(4)	N(13)–Ni(1)–O(1)	90.6(5)
N(24)–Ni(2)–N(21)	178.5(4)	N(13)–Ni(1)–N(11)	90.7(3)
N(24)–Ni(2)–N(22)	92.3(5)	N(13)–Ni(1)–N(12)	174.9(3)
N(24)–Ni(2)–N(23)	86.3(4)	N(14)–Ni(1)–Cl(1)	88.7(3)
O(1)–Ni(1)–Cl(1)	177.2(4)	N(14)–Ni(1)–O(1)	89.3(4)
N(11)–Ni(1)–Cl(1)	95.7(2)	N(14)–Ni(1)–N(11)	174.3(4)
N(11)–Ni(1)–O(1)	86.4(3)	N(14)–Ni(1)–N(12)	99.4(4)
N(12)–Ni(1)–Cl(1)	89.6(3)	N(14)–Ni(1)–N(13)	85.6(3)
N(12)–Ni(1)–O(1)	88.7(5)		

Table 6 Fractional atomic coordinates (× 10^5 for Ni and Cl, × 10^4 for others) for $[(NiCl_2)_2(tabm)]{\cdot}2H_2O$ with e.s.d.s in parentheses

Atom	*X/a*	*Y/b*	*Z/c*
Ni(1)	69 231(8)	10 301(3)	−2 787(10)
Ni(2)	63 511(8)	39 305(3)	26 196(10)
Cl(11)	49 859(19)	8 202(6)	17 753(22)
Cl(12)	88 997(19)	12 273(8)	−23 088(23)
Cl(21)	45 283(18)	39 670(7)	−9 327(22)
Cl(22)	81 263(19)	39 679(8)	62 218(22)
N(11)	5 798(5)	1 820(2)	−1 005(6)
N(12)	5 246(6)	627(2)	−2 975(7)
N(13)	8 512(5)	1 460(2)	2 439(7)
N(14)	8 098(6)	257(2)	542(7)
N(21)	5 526(5)	3 015(2)	2 538(7)
N(22)	4 440(6)	4 106(2)	3 861(8)
N(23)	8 152(5)	3 696(2)	1 291(7)
N(24)	7 307(6)	4 826(2)	2 643(8)
C(1)	7 870(6)	2 546(2)	1 676(8)
C(2)	6 891(6)	2 393(2)	−614(8)
C(3)	4 813(7)	1 702(3)	−3 191(8)
C(4)	3 972(7)	1 053(3)	−3 558(8)
C(5)	9 159(6)	2 092(2)	2 434(8)
C(6)	9 870(7)	1 061(3)	3 033(8)
C(7)	9 115(8)	399(3)	2 712(9)
C(8)	6 773(6)	2 580(2)	3 101(8)
C(9)	4 440(7)	3 003(3)	3 883(9)
C(10)	3 374(7)	3 527(3)	3 479(9)
C(11)	8 982(6)	3 144(2)	1 898(8)
C(12)	9 359(7)	4 238(3)	1 738(9)
C(13)	8 445(8)	4 805(3)	1 352(10)
O(1)	2 336(7)	2 171(3)	−553(10)
O(2)	1 130(7)	3 190(3)	−2 437(11)

constant studies[50] indicate that cyclam adapts exceptionally well to both low- and high-spin nickel(II) ions. While there is no structural information available for the nickel(II) complexes of both 3,7-diazanonane-1,9-diamine and 4,7-diazadecane-1,10-diamine, the acyclic analogues of cyclam, such information is now available for tabm and its macrocyclic analogue, C-spirobicyclam.[21]

The data for Ni–N distances used in predicting a 'best fit' Ni–N distance for low-spin nickel(II) complexes are presented in Table 8. Although, there are diverse structural aspects of the ligands involved, an indication is provided of how different factors can lead to variation of Ni–N distances in low-spin nickel complexes. For example, in the complex cations $[Ni(Me_2[13]aneN_4)]^{2+}$ ($Me_2[13]aneN_4$ = 12,12-dimethyl-1,4,7,10-tetraazacyclotridecane)[41] and $[Ni(trien)]^{2+}$ (trien = 3,6-diazaoctane-1,8-diamine)[42] three adjacent five-membered chelate rings are present and hence the ligands may not be in a completely strain-free configuration.

Table 7 Interatomic distances (Å) and angles (°) for $[(NiCl_2)_2(tabm)]{\cdot}2H_2O$ with e.s.d.s in parentheses

Cl(11)–Ni(1)	2.508(2)	Cl(21)–Ni(2)	2.502(2)
Cl(12)–Ni(1)	2.519(2)	Cl(22)–Ni(2)	2.494(2)
N(11)–Ni(1)	2.085(4)	N(21)–Ni(2)	2.091(4)
N(12)–Ni(1)	2.079(4)	N(22)–Ni(2)	2.097(5)
N(13)–Ni(1)	2.077(4)	N(23)–Ni(2)	2.079(4)
N(14)–Ni(1)	2.083(5)	N(24)–Ni(2)	2.092(5)
Cl(12)–Ni(1)–Cl(11)	179.0(1)	N(23)–Ni(2)–Cl(22)	94.4(1)
N(11)–Ni(1)–Cl(11)	87.8(1)	N(23)–Ni(2)–N(21)	91.9(2)
N(11)–Ni(1)–Cl(12)	93.2(1)	N(23)–Ni(2)–N(22)	175.8(2)
N(12)–Ni(1)–Cl(11)	91.5(1)	N(24)–Ni(2)–Cl(21)	90.0(1)
N(12)–Ni(1)–Cl(12)	88.9(1)	N(24)–Ni(2)–Cl(22)	87.0(1)
N(12)–Ni(1)–N(11)	84.6(2)	N(24)–Ni(2)–N(21)	176.2(2)
N(13)–Ni(1)–Cl(11)	86.8(1)	N(24)–Ni(2)–N(22)	99.5(2)
N(13)–Ni(1)–Cl(12)	92.8(1)	N(24)–Ni(2)–N(23)	84.4(2)
N(13)–Ni(1)–N(11)	93.1(2)	Cl(22)–Ni(2)–Cl(21)	176.0(1)
N(13)–Ni(1)–N(12)	177.2(2)	N(21)–Ni(2)–Cl(21)	90.5(1)
N(14)–Ni(1)–Cl(11)	92.0(2)	N(21)–Ni(2)–Cl(22)	92.7(1)
N(14)–Ni(1)–Cl(12)	87.0(2)	N(22)–Ni(2)–Cl(21)	90.4(1)
N(14)–Ni(1)–N(11)	178.0(2)	N(22)–Ni(2)–Cl(22)	87.5(1)
N(14)–Ni(1)–N(12)	97.4(2)	N(22)–Ni(2)–N(21)	84.3(2)
N(14)–Ni(1)–N(13)	84.9(2)	N(23)–Ni(2)–Cl(21)	87.9(1)

Table 8 Bond lengths (Å) in selected square-planar nickel(II) amine complexes

Complex	Average Ni–N distance	Ref.
1 $[Ni(daco)_2][ClO_4]_2$	1.945(3)[a]	36
2 $[Ni(cyclam)][ClO_4]_2$	1.955(2)[a]	37
3 $[Ni(cyclam)][ClO_4]_2$	1.975(2)[a]	37
4 $[Ni(isocyclam)][ClO_4]_2$[b]	1.988(13)[a]	38
5 $[Ni(cyclam)]I_2$	1.95(1)[a]	39
6 $[Ni(HL^2)][I_3]I_2$	1.929(8)[a]	40
7 $[Ni_2(tabm)][ClO_4]_4{\cdot}H_2O$	1.927(12)[a] 1.924(10)[a]	This work
8 $[Ni_2(L^1)][ClO_4]_4$	1.948(7)[a] 1.933(8)[a]	21
9 Various macrocyclic complexes of Ni^{II}	1.943(29)[a]	27
10 $[Ni(Me_2[13]aneN_4)]^{2+}$[c]	1.863(20)	41
11 $[Ni(trien)]^{2+}$[c]	1.885 1.925	42
12 $[Ni(diaminostilbene)_2]^{2+}$[c]	1.89	43
13 $[Ni(cyclam)Cl_2]$[d]	2.067(1)	44
14 $[Ni(cyclam)(NCS)_2]$[d]	2.074	45

[a] Used to obtain mean value for Ni–N bond [1.945(29) Å]. [b] Isocyclam = 1,4,7,11-tetraazacyclotetradecane. [c] Used to calculate an ideal Ni–N bond length of 1.89 Å. [d] Included to provide a comparison between the bond lengths in square-planar and octahedral nickel(II) complexes.

An interesting result is the exact agreement between the mean Ni–N distance [1.945(29) Å] calculated from most of the complexes in Table 8 and the reported bond length in $[Ni(daco)_2]^{2+}$ [1.945(3) Å] (daco = 1,5-diazacyclooctane).[36] In $[Ni(daco)_2]^{2+}$ the methylene linkages sterically protect the axial position and the lack of an 'in-plane' carbon framework permits the metal–nitrogen distance to vary unrestrained. Hence, this ion may represent the archetypal low-spin square-planar nickel(II) complex.

The crystal structures[21] of $[Ni_2(tabm)]^{4+}$ and $[Ni_2L^1]^{4+}$ provide an interesting comparison between an acyclic precursor and its macrocyclic analogue. The only difference between these cations is the additional six-membered ring closing the macrocyclic complex. This ring does not appear to alter significantly the bond lengths and angles within the ligand nor the Ni–N bond lengths and angles in the co-ordination sphere. The small changes in the bond lengths are presumably a result of the conversion of a primary into a secondary amine and the

Table 9 Ultraviolet–visible spectroscopic data for nickel(II) complexes

Complex	Medium	λ_{max}/nm(ε/dm^3 mol^{-1} cm^{-1})
$[(NiCl_2)_2(tabm)]\cdot 2H_2O$	Water	344(14.0), 448(6.0), 740(5.3), 785(5.0)
$[Ni_2(tabm)][ClO_4]_4\cdot H_2O$	Water	345(17.4), 448(9.2), 537(10.0), 742(8.0), 787.1(7.5)
	80% EtOH	345(17.7), 453(6.6), 537(9.9), 742(8.0), 787(7.3)
	6 mol dm^{-3} $NaClO_4$	448.4(74.2)
	MeCN	337(14.8), 510(9.0), 747(8.2), 790(7.6)
	$MeNO_2$	448(96.6)
$[Ni_2Cl(OH_2)(tabm)][ClO_4]_3\cdot H_2O$	Water	345(26.8), 445(7.6), 536(8.2), 740(7.6), 786(7.0)
	MeCN	342(31.7), 526(13.0), 747(9.7)
	$MeNO_2$	450(63.0), 557(19.6)

Table 10 Thermodynamic parameters for the square planar $\rightleftharpoons$ octahedral equilibrium for various nickel(II) complexes of tetraaza ligands

Ligand	% Square planar	ΔH/ kcal mol^{-1}	ΔS/cal K^{-1} mol^{-1}	Ref.
L^3*	22.0	3.4	9.0	45
HL^2	7.2	4.4	9.7	46
tabm	11.8	4.2	10.2	This study

* 3,7-Diazanonane-1,9-diamine.

chelate angle imposed by the six-membered ring. The relatively small geometry changes appear to argue against any significant contraction of the bonds in forming the macrocyclic complex. Indeed, a slight expansion of the Ni–N bonds occurs and a constrictive effect of the macrocyclic ligand would not seem to be a plausible explanation for the macrocyclic effect.

Synthesis.—We reported recently studies of the reaction of pentaerythrityl tetrabromide with ethylenediamine and the separation of the mixture of product amines *via* nickel(II) complexation.[26] The nickel(II) complex of tabm described in this report was isolated as the major product. Our primary interest was to isolate tabm in good yields and a pure form in order to permit the synthesis and investigation of the homo- and hetero-binuclear complexes of its macrocyclic analogue, C-spiro-bicyclam(L^1).[21]

In an earlier report Philip[22] described the preparation of this ligand and the properties of its nickel(II) and palladium(II) complexes. From ultraviolet–visible spectroscopic studies it was concluded that in the binuclear palladium(II) complex both metal centres adopted a square-planar geometry. However, in the case of the nickel(II) complex one of the metal centres was proposed to exist as a NiN_6 chromophore (nickel ion bound by three of the four arms of tabm as shown in structure **II**) and the other was considered to be an NiN_2O_2 chromophore in which the oxygen donors were water molecules and the nitrogens from the remaining arm of tabm. Recently Gahan *et al.*[25] described similar methods for the preparation of tabm and reported the properties and structural characterisation of a binuclear copper(II) complex. Under appropriate conditions, it has been shown possible to isolate a mononuclear cobalt(III) complex containing a $Co^{III}N_6$ unit and the structural characterisation of its cage-type derivative has been reported.[24] In the present studies, an excess of nickel salt was used during the isolation of tabm[26] and hence only binuclear complexes were isolated.

In both solution and the solid state, the co-ordination geometry adopted by a nickel(II) centre depends upon a number of factors such as temperature, ionic strength, solvent and co-ordinating ability of the counter ions. Evidence for the existence of the various binuclear geometries in solution is provided by ultraviolet–visible and electrochemical studies (see below).

Ultraviolet–Visible Spectroscopy.—Ultraviolet–visible spectra of all three complexes have been studied in various solvents and data are presented in Table 9. The behaviour of these complexes differs significantly with the varying media used.

In aqueous solution there is an equilibrium mixture of the square-planar and the octahedral species. However, as a result of variations in the counter ions, a small noticeable difference in the composition of these equilibrium mixtures is observed. These equilibria show both a temperature and ionic strength dependence, behaviour reminiscent of many other nickel(II) complexes of tetraaza ligands such as 3,7-diazanonane-1,9-diamine.[51]

The bands at 450 and 537 nm, observed in aqueous media, are characteristic of the square-planar and octahedral species respectively. Although the spectra of these complexes exhibit features comparable to those of 3,7-diazanonane-1,9-diamine[23] and similar ligands [*e.g.* 6,6′-bis(4-amino-2-azabutyl)-1,4-diazacycloheptane(L^2)[40]] under identical conditions (25 °C, 0.1 mol dm^{-3} $NaClO_4$ in water), the relative ratios of square-planar to octahedral species are different (see Table 10). This is not reflected in the thermodynamic parameters for the square planar $\rightleftharpoons$ octahedral equilibrium. The significantly lower percentage of the square-planar species which is observed in the case of $[Ni_2(tabm)]^{4+}$ and $[Ni(HL^2)]^{3+}$ can be attributed to the electrostatic repulsion between the cationic centres within the same molecule.

Though the complex cations of tabm show nearly identical ultraviolet–visible spectra in aqueous media, they can be distinguished clearly in acetonitrile and nitromethane. In the former, $[Ni_2(tabm)]^{4+}$ dissolves to form a pink solution species which shows an absorption band at 510 nm, characteristic of pseudo-octahedral nickel(II) centres. Contrary to its behaviour in aqueous media, the spectrum of $[Ni_2(tabm)]^{4+}$ in acetonitrile shows no temperature dependence, with only the octahedral species present. In contrast, the macrocyclic cation $[Ni_2L^1]^{4+}$ in acetonitrile exhibits a square-planar $\rightleftharpoons$ octahedral equilibrium. Previously, in a similar study on the nickel(II) complexes of 3,7-diazanonane-1,9-diamine, 4,6-diazadecane-1,10-diamine and cyclam in aqueous media, Fabbrizzi and co-workers[51] concluded that macrocyclisation is not a controlling factor in such equilibria. However, from comparison of the behaviour of nickel(II) complexes of 3,7-diazanonane-1,9-diamine with cyclam and of tabm with L^1 (C-spiro-bicyclam) in acetonitrile there is clear evidence that macrocyclisation is a factor. In spite of their structural resemblances, in the nickel(II) complex of tabm the chelate rings are more rigid than in the complex of 3,7-diazanonane-1,9-diamine. This accounts for the kinetic inertness and the ease of formation of the nickel(III) species (see below) in both aqueous and non-aqueous media. However, the chelating arms are still flexible enough in the NiN_4 plane to accommodate the changes in the Ni–N bond lengths during the formation of high-spin octahedral complexes.

The complex cation $[Ni_2Cl(OH_2)(tabm)]^{3+}$ in acetonitrile shows a single broad band at 526 nm with no temperature dependence. The feature is believed to comprise both a band observed for the $[Ni_2(tabm)]^{4+}$ cation at 510 nm and a second

Table 11 Ultraviolet–visible spectroscopic data for nickel(III) species in solution

Nickel(III) species/medium	λ_{max}/nm (ε/dm^3 mol^{-1} cm^{-1})
All three cations oxidised in aqueous 4.0 mol dm^{-3} NaCl with $K_2S_2O_8$	271 (1.73 × 10^4), 317 (1.8 × 10^4)
$[Ni_2(tabm)]^{4+}$ in MeCN	
a	216 (4.0 × 10^4), 283 (8.0 × 10^3), 325 (4.0 × 10^3)
b	238(br) (1.2 × 10^5), 324(sh) (470), 452(sh) (87), 619(sh) (39), 643 (51), 702 (52)

[a] Oxidised by $NOBF_4$. [b] Oxidised by $NOBF_4$ in the presence of chloride.

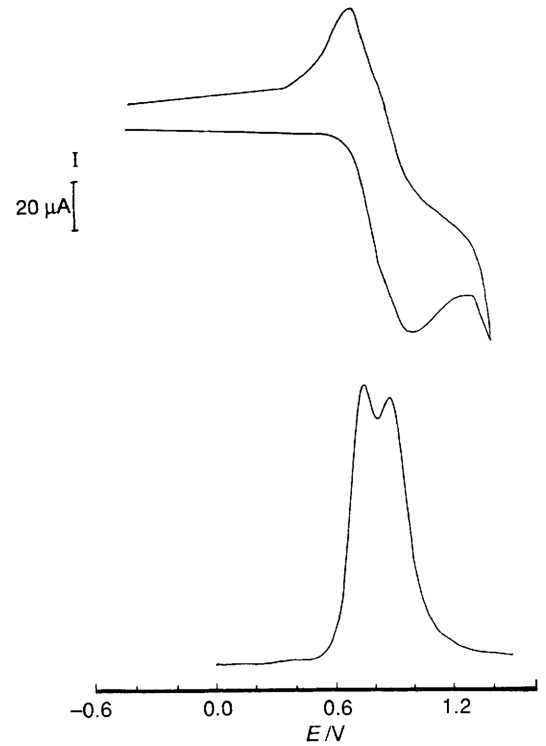

Fig. 4 Cyclic voltammogram and differential pulse polarogram of $[Ni_2(tabm)]^{4+}$ in MeCN (0.1 mol dm^{-3} NEt_4BF_4), Ag–Ag$^+$ reference electrode, scan rate 2 mV s^{-1}

absorption from the other octahedral centre. This indicates that the original square-planar nickel(II) centre is not present in this solvent.

In the poorly co-ordinating solvent nitromethane the cation $[Ni_2(tabm)]^{4+}$ exists only in the square-planar form (see Table 9). This provides a limiting ε value of 96.6 dm^3 mol^{-1} cm^{-1} which is typical for two square-planar nickel(II) centres and is comparable to a value of 74.2 dm^3 mol^{-1} cm^{-1} observed in saturated sodium perchlorate solutions. The cation with one square-planar and one octahedral nickel centre retains its structural integrity in $MeNO_2$ media. Two distinct bands at 557 and 450 nm corresponding to the octahedral and square-planar nickel(II) centres are observed with appropriate absorption coefficients (see Table 9). The neutral complex $[(NiCl_2)_2(tabm)]$ is only very sparingly soluble in nitromethane and acetonitrile. Hence, its physical properties were not studied in detail in these solvents.

Ultraviolet–visible spectra of the nickel(III) species generated in both aqueous and acetonitrile media were studied and the spectroscopic data are presented in Table 11. The features close to 310 and 217 nm are typical of nickel(III) species comprising tetraaza ligands.[52] The spectrum of the nickel(III) species showed a significant dependence on chloride concentration. Studies of the oxidation of $[Ni_2(tabm)]^{4+}$ in MeCN show distinct differences in the presence and absence of Cl^-. Whereas there are no marked features above 600 nm in the former case, when Cl^- is present, d–d bands were observed at 619, 643 and 702 nm which are unlikely to correspond to a single species.

Electrochemical Studies.—Cyclic voltammograms of cations $[Ni_2(tabm)]^{4+}$, $[(NiCl_2)_2(tabm)]$ and $[Ni_2Cl(OH_2)(tabm)]^{3+}$ were obtained in aqueous media. All three cations showed similar behaviour. In 0.1 mol dm^{-3} $LiClO_4$ only one quasi-reversible wave was observed at potentials close to the solvent limits. Addition of chloride improved the reversibility due to stabilisation of the nickel(III) species through formation of the bis(dichloro) complex. In 1.0 mol dm^{-3} NaCl ($[H^+]$ = 0.1 mol dm^{-3}) a single quasi-reversible wave was observed for the Ni^{II}–Ni^{III} couple with $E_{\frac{1}{2}} \approx 0.710$ V *vs.* ferrocene–ferrocenium. The variations of E_{pa} and E_{pc} with scan rate were distinctly different suggesting a form of kinetic dependence. This observation implies that the successive transfer of one electron from each nickel centre is followed by a chemical reaction, presumably substitution. However, substitution rates differ for the nickel-(II) and -(III) species as evidenced by a complex behaviour for the oxidation and reduction waves. Owing to the quasi-reversible nature and the observed form of the waves it was not possible to evaluate the individual redox potentials.

The electrochemistry of the neutral complex $[(NiCl_2)_2(tabm)]$ was not studied in non-aqueous media because of its poor solubility. Also, the complex precipitated in the presence of electrolytes. However, the cations $[Ni_2(tabm)]^{4+}$ and $[Ni_2Cl(OH_2)(tabm)]^{3+}$ form stable solutions in acetonitrile. The cyclic voltammogram of $[Ni_2(tabm)]^{4+}$ (0.1 mol dm^{-3} NEt_4BF_4) showed two waves indicating consecutive transfer of one electron from each of the nickel centres: $[Ni^{II}_2(tabm)]^{4+} \xrightarrow{-e} [Ni^{II}Ni^{III}(tabm)]^{5+} \xrightarrow{-e} [Ni^{III}_2(tabm)]^{6+}$. Under identical conditions, two well resolved oxidation peaks were observed by differential pulse polarography (Fig. 4). The individual redox potentials were estimated to be 860 and 960 mV respectively.[46] From these $E_{\frac{1}{2}}$ values, the comproportionation constant $[K_c = \exp(\Delta E_{\frac{1}{2}} n_1 n_2 F/RT)]$ for the mixed-valence intermediate species was estimated to be 72.5. The cyclic voltammogram of the cation $[Ni_2Cl(OH_2)(tabm)]^{3+}$ in acetonitrile showed a complex wave pattern.

ESR Spectroscopy.—All three cations can be oxidised to nickel(III) species in neutral aqueous media by $S_2O_8^{2-}$ and in acetonitrile using $NOBF_4$. Oxidation is observed also by reagents such as nickel(III) ion in 1.0 mol dm^{-3} $HClO_4$, but, owing to the instability of the nickel(II) cations in acid, a reagent at neutral pH is preferred.

Upon oxidation with sodium peroxodisulphate five features at g = 2.279, 2.215, 2.149, 2.072 and 2.022 were observed [Fig. 5(*a*)]. On standing, the intensities of signals at g = 2.215 and 2.022 increased, but the final spectrum still exhibited all five g components. Upon addition of chloride ($\approx$0.25 mol dm^{-3}) there was a shift in some peak positions (see Fig. 5). Hyperfine splitting was observed for g = 2.022 [Fig. 5(*b*)]. By comparison with nickel(III) complexes of other tetraaza macrocycles,[52] the peaks observed at 2.180 (g_{xx}, g_{yy}) and 2.022 (g_{zz}, $A_{\parallel}$ = 28.5 G) were assigned to the presence of an axially symmetric nickel(III) centre with chlorides as *trans*-axial ligands. The expected septet due to the two chloride ions cannot be seen clearly owing to overlapping of the absorption at 2.066. However, on standing, the three peaks at 2.236, 2.117 and 2.066 gradually diminished such that a septet pattern could be observed. The changes are thought to result from the slow substitution of chloride into the sulphato complexes derived from peroxodisulphate.

It is not possible to assign with certainty the three

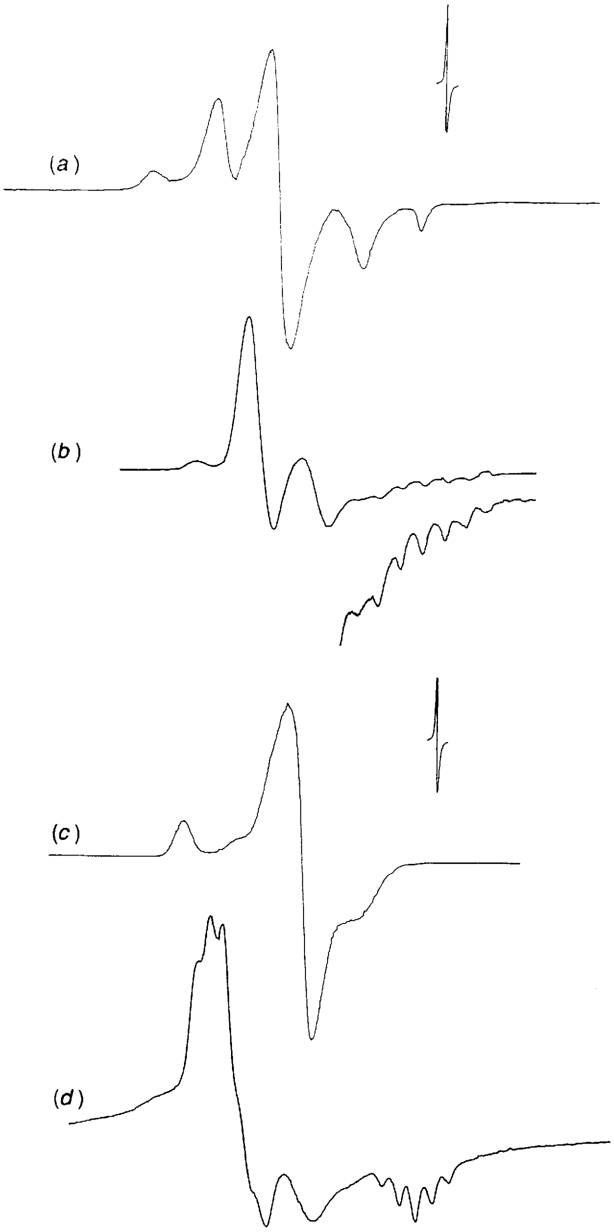

Fig. 5 ESR spectra of species derived on oxidation of $[Ni_2(tabm)]^{4+}$: (*a*) green solution formed immediately on reaction with $S_2O_8^{2-}$ in aqueous media; (*b*) as above after 25 min and addition of 0.2 mol dm^{-3} NaCl; (*c*) oxidation by $S_2O_8^{2-}$ in saturated NaCl; and (*d*) oxidation by NO^+ in MeCN in the presence of $MeNO_2$

absorptions at $g = 2.236$, 2.117 and 2.066 to a particular geometry for the nickel(III) centres (see below). However, when the nickel(III) species was generated at high chloride concentrations (> 4.0 mol dm^{-3}) an anisotropic spectrum with only *g* components at 2.236, 2.117 and 2.067 was observed [Fig. 5(*c*)]. This species did not undergo any spectral changes during a much slower decomposition.

The spectrum shown in Fig. 5(*c*) suggests that both nickel(III) centres adopt an identical geometry (possibly five-co-ordinate) in which each is present in an anisotropic environment. However, when diluted (at least 50 times), on standing the slow appearance of an axially symmetrical species was observed with some decomposition. The experimental observations indicate that the tetragonal nickel(III) species is not originally present in solution and is formed from another anisotropic species. In aqueous media all three cations showed similar behaviour on oxidation.

In acetonitrile, the nickel(III) species generated from all three cations showed behaviour essentially similar to that observed in aqueous media [*i.e.* initially forming a nickel(III) species which slowly rearranged to a species with tetragonal geometry]. On oxidation, the cation $[Ni_2(tabm)]^{4+}$ formed a nickel(III) species with nitrogen donors as axial ligands ($g_\perp = 2.198$, $A_\perp = 15$ G, $g_\parallel = 2.022$, $A_\parallel = 21.3$ G) [Fig. 5(*d*)] demonstrated by the quintet splitting of the $g_\parallel$ and $g_\perp$ components. Upon addition of tetrabutylammonium chloride the weakly bound axial ligand was replaced by chloride ions and hyperfine splitting ($g_\perp = 2.151$, $g_\parallel = 2.004$, $A_\parallel = 30$ G) due to chloride was observed instantaneously.

While the nickel(II) centres in the complex of tabm can adopt octahedral geometry without much steric constraint, on oxidation to Ni^{III} the contraction of axial bonds could induce steric effects leading to distinct distortions from octahedral geometry. The extent of this induced steric effect also depends on the steric bulkiness of the axial ligand.

The electrochemical behaviour parallels the spectroscopic observations on the nickel-(II) and -(III) species present in solution. The composition of the nickel(II) species is known from ultraviolet–visible spectroscopic studies and that of the nickel(III) species from ESR measurements. During the oxidation scan the equilibrium mixture of square-planar and octahedral nickel(II) species present in aqueous solution is oxidised to form a mixture of nickel(III) species, which further undergo substitution at axial sites. During the reduction scan the nickel(III) species are reduced to Ni^{II} with subsequent rearrangement. Hence, the overall process can be considered as an electrochemical–chemical–electrochemical–chemical (e.c.e.c.) process[53] which occurs successively over the two nickel centres.

However, the rates of substitution of ligands on the nickel-(II) and -(III) centres are significantly different. The equilibrium between the square-planar and octahedral nickel(II) species has been shown to be sensitive to the anion present, the temperature and the solvent. Although the nickel complexes in aqueous media may be described as a mixture of square-planar and octahedral species, a series of intermediate geometries is possible. The nature of the nickel(III) species formed depends largely upon the initial equilibrium mixture involving the various nickel(II) ions.

In acetonitrile media the $[Ni_2(tabm)]^{4+}$ cation dissolves to form a single bis(octahedral) species. During oxidation the nickel centres undergo very little change in geometry. As a result two separate waves of equal height are observed in the electrochemical experiments, corresponding to the successive oxidation of nickel centres. In electrochemical terms, this can be described as an e_re_r (electron reversible, electron reversible) type of process.[53] The ESR spectrum of the Ni^{III}_2 species generated from $[Ni_2(tabm)]^{4+}$ obtained in acetonitrile (both in the presence and absence of chloride) confirms the octahedral geometry of this species.

Finally, the possibility of generating and identifying the mixed-valence Ni^{II}Ni^{III} species needs further consideration. In both aqueous and acetonitrile media the nickel centres undergo successive oxidations. In the former, the geometry change that accompanies the first oxidation reduces electrostatic repulsion and hence facilitates oxidation of the second nickel centre. In acetonitrile, both nickel centres exist in octahedral geometry and the redox potentials for the successive oxidations of the nickel(II) centres are 100 mV apart. This difference is not large enough to isolate the mixed-valence species in appreciable concentrations.

Acknowledgements

The authors would like to thank the Natural Sciences and Engineering Research Council (Canada) and the University of Victoria for financial support. The award of Fellowships (T. W. W., NSERC; S. S., University of Victoria) is also acknowledged.

References

1 D. E. Fenton, *Adv. Inorg. Bioinorg. Mech.*, 1983, **2**, 187.

2 R. R. Gagne, C. A. Koval, T. J. Smith and M. C. Cimolino, *J. Am. Chem. Soc.*, 1979, **101**, 4571 and refs. therein.

3 U. Casellato and P. A. Vigato, *Coord. Chem. Rev.*, 1977, **23**, 31.

4 M.-T. Youinou, J. A. Osborne, J.-P. Collin and P. Lagrange, *Inorg. Chem.*, 1986, **25**, 453.

5 C. A. Salata, D. V. Engen and C. J. Burrows, *J. Chem. Soc., Chem. Commun.*, 1988, 579.

6 A. W. Maverick and F. E. Klavetter, *Inorg. Chem.*, 1984, **23**, 4129; A. W. Maverick, S. C. Buckingham, Q. Yao, J. R. Bradbury and G. G. Stanley, *J. Am. Chem. Soc.*, 1986, **108**, 7430.

7 N. A. Bailey, M. M. Eddy, D. E. Fenton, G. Jones, S. Moss and A. Mukhopadhyay, *J. Chem. Soc., Dalton Trans.*, 1981, 628.

8 J. Nelson, B. P. Murphy, M. G. B. Drew, P. C. Yate and S. M. Nelson, *J. Chem. Soc., Dalton Trans.*, 1988, 1001.

9 J.-M. Lehn, *Pure Appl. Chem.*, 1980, **52**, 2441.

10 I. Murase, S. Ueno and S. Kida, *Inorg. Chim. Acta*, 1986, **111**, 37.

11 M. W. Makinen, S. A. Schichman, S. C. Hill and H. B. Gray, *Science*, 1983, **222**, 929.

12 R. L. Lintvedt in *Copper Coordination Chemistry: Biochemical and Inorganic Perspectives*, eds. K. D. Karlin and J. Zubieta, Adenine Press, New York, 1983.

13 M. N. Bell, A. J. Blake, M. Schroder and T. A. Stephenson, *J. Chem. Soc., Chem. Commun.*, 1986, 471; A. McAuley, T. W. Whitcombe and M. J. Zaworotko, *Inorg. Chem.*, in the press.

14 K. Wieghardt, I. Tolksdorf and W. Herrmann, *Inorg. Chem.*, 1985, **24**, 1230.

15 R. Schneider, A. Riesen and Th. A. Kaden, *Helv. Chim. Acta*, 1986, **69**, 53.

16 L. Fabbrizzi, F. Forlani, A. Perotti and B. Seghi, *Inorg. Chem.*, 1984, **23**, 807.

17 T. L. Netzel, M. A. Bergkamp and C. K. Chang, *J. Am. Chem. Soc.*, 1982, **104**, 1952.

18 R. E. Overfield, A. Scherz, K. J. Kaufmann and M. R. Wasielewski, *J. Am. Chem. Soc.*, 1983, **105**, 5747.

19 A. Osuka, K. Maruyama, I. Yamazaki and N. Tamai, *J. Chem. Soc., Chem. Commun.*, 1988, 1243 and refs. therein.

20 A. Buttafava, L. Fabbrizzi, A. Perotti and B. Seghi, *J. Chem. Soc., Chem. Commun.*, 1982, 1166.

21 A. McAuley, S. Subramanian and T. W. Whitcombe, *J. Chem. Soc., Chem. Commun.*, 1987, 539.

22 A. T. Philip, *Aust. J. Chem.*, 1968, **21**, 2301.

23 B. Bosnich, R. D. Gillard, E. D. Mckenzie and G. A. Webb, *J. Chem. Soc. A*, 1966, 1331.

24 A. A. Achilleos, L. R. Gahan, K. A. Nicolaidis and T. W. Hambley, *J. Chem. Soc., Chem. Commun.*, 1988, 912.

25 L. R. Gahan, K. E. Hart, C. H. L. Kennard, M. A. Kingston, G. Smith and T. C. W. Mak, *Inorg. Chim. Acta*, 1986, **116**, 5.

26 A. McAuley, K. Beveridge, S. Subramanian and T. W. Whitcombe, *Can. J. Chem.*, 1989, **67**, 1657.

27 K. Henrick, P. A. Tasker and L. F. Lindoy, *Prog. Inorg. Chem.*, 1985, **33**, 1.

28 R. D. Hancock, *Pure Appl. Chem.*, 1986, **58**, 1445.

29 L. J. Fabbrizzi, *J. Chem. Soc., Dalton Trans.*, 1979, 1857.

30 G. M. Sheldrick, SHELX 76, Program for crystal structure refinement, University of Cambridge, 1976.

31 D. T. Cromer and J. B. Mann, *Acta Crystallogr., Sect. A*, 1968, **24**, 321.

32 *International Tables for X-Ray Crystallography*, Kynoch Press, Birmingham, 1974, vol. 4.

33 P. Coppens, L. Lieserowitz and D. Rabinovich, modified by G. W. Bushnell, University of Victoria, 1978.

34 P. Main, MULTAN, University of York, 1978.

35 R. R. Gagne, C. A. Koval and G. C. Lisenky, *Inorg. Chem.*, 1980, **19**, 2854.

36 D. J. Royer, V. H. Schievelbein, A. Kalyanaraman and J. A. Bertrand, *Inorg. Chim. Acta*, 1972, **6**, 307.

37 L. Prasad, S. C. Nyburg and A. McAuley, *Acta Crystallogr., Sect. C*, 1987, **43**, 1038; T. W. Whitcombe and A. McAuley, unpublished work.

38 J. C. A. Boeyens, *Acta Crystallogr., Sect. C*, 1983, **39**, 846.

39 A. McAuley, unpublished work.

40 A. McAuley and S. Subramanian, *Inorg. Chem.*, 1991, **30**, 371.

41 J. M. Waters and K. R. Whittle, *J. Inorg. Nucl. Chem.*, 1972, **34**, 155.

42 A. C. McPherson, M. G. Rossman, D. W. Margerum and M. R. J. James, *J. Co-ordination Chem.*, 1971, **1**, 39.

43 S. C. Nyburg and J. S. Wood, *Inorg. Chem.*, 1964, **3**, 468.

44 B. Bosnich, R. Mason, P. J. Pauling, G. B. Robertson and M. L. Tobe, *Chem. Commun.*, 1965, 95.

45 T. Ito, M. Kato and H. Ito, *Bull. Chem. Soc. Jpn.*, 1984, **57**, 2641.

46 D. E. Richardson and H. Taube, *Inorg. Chem.*, 1981, **20**, 1279.

47 N. M. N. Gowda, S. B. Naikar and G. K. N. Reddy, *Adv. Inorg. Chem. Radiochem.*, 1984, **28**, 255.

48 See, for example, K. Barefield, A. Bianchi, E. J. Billo, P. J. Connolly, P. Paoletti, J. S. Summers and D. G. Van Derver, *Inorg. Chem.*, 1986, **25**, 4197.

49 M. D. Glick, R. L. Lintvedt, T. J. Anderson and J. L. Mack, *Inorg. Chem.*, 1976, **15**, 2258.

50 D. Hinz and D. W. Margerum, *Inorg. Chem.*, 1974, 13, 2941; see also ref. 15 in R. D. Hancock and A. E. Martell, *Comments Inorg. Chem.*, 1988, **6**, 237.

51 A. Anchini, L. Fabbrizzi, P. Paoletti and R. M. Clay, *Inorg. Chim. Acta*, 1977, **24**, L21.

52 R. I. Haines and A. McAuley, *Coord. Chem. Rev.*, 1981, **39**, 77.

53 A. J. Bard and L. R. Faulkner in *Electrochemical Methods*, Wiley, New York, 1980, ch. 11.

Received 18*th December* 1990; *Paper* 0/05685E